35th Annual International Conference of the IEEE EMBS
Osaka, Japan, 3 - 7 July, 2013

Cardiac PET Imaging of ^{18}F-FDG Metabolism: Study of Healthy and Infarcted Hearts of Rats

R. Mabrouk[1, 2], F. Dubeau[3], and L. Bentabet[4]

Abstract—**This paper, considers the evolution of a method presented previously by authors to correct for cross contamination effect on the dynamic image sequences and shows how this development allows for a robust voxel by voxel implementation yielding parametric images for healthy and unhealthy subjects. Our approach is based on the decomposition of image pixel intensity into blood and tissue components using Bayesian statistics. The method uses an *a priori* knowledge of the probable distribution of blood and tissue in the images. Likelihood measures are computed by a General Gaussian Distribution (GGD) model. Bayes' rule is then applied to compute weights that account for the concentrations of the radiotracer in blood and tissue and their relative contributions in each image pixel. We tested the method on a set of dynamic cardiac ^{18}F-fluoro-deoxy-d-glucose PET of healthy rats and unhealthy rats. The results show the benefit of our correction on the generation of parametric images of myocardial metabolic rates for glucose (MMRG).**

Keywords: PET, Kinetic Modeling, Input Function, Bayes Rule.

I. Introduction

Imaging of myocardial viability by PET is a medical exam to assess glucose metabolism of the heart. The objective is to evaluate cells damaged or destroyed by heart disease through rate of glucose metabolism. The use of images allows both to confirm the cardiac lesions revealed by another investigation and to assess the extent of tissue damage following a heart disease. The estimation of the MMRG from PET images is obtained by compartmental modeling. This method uses image data but requires an input function (IF) to account for the radiotracer delivered to the tissue.

Up to now, the invasive gold standard arterial plasma sampling procedure to obtain IF remains the reference. An alternative method has been developed to extract IF directly from image sequences [1-2].

In this paper, we improve the approach presented in [3] based on the decomposition of the pixel intensity of blood and tissue components. The likelihood function in this work is estimated from the spatial domain modeled by a GGD.

Manuscript received January 18, 2013.
Corresponding author: Rostom Mabrouk.
Email addresses: rostom.mabrouk@usherbrooke.ca, Tel.: +1 189 346-1110 ext 13152; fax: +1 819 564-5440.
(1) Computer Sciences Department.
(2) Nuclear Medicine Department, Université de Sherbrooke (Qc).
(3) Mathematics Department Université de Sherbrooke (Qc).
(4) Computer Sciences Department, Bishop's University

II. Materials and Methods

A. PET measurements

All experiments were performed on Fischer male rats weighing 200−220 g (Charles River Canada). The experiments followed a protocol approved by the Canadian Council on Animal Care and the in-house ethics committee. The experimental protocol was designed in such a way that the animals had free access to food and water throughout the studies. The study was performed on a set of normal rats (n=12) and rats with myocardial infarcted (MI) induced by ligature of the left coronary artery (n=4) injected by the ^{18}F-Fluoro-Deoxy -Glucose (^{18}F-FDG). The PET scans were performed with the Sherbrooke small-animal PET scanner (LabPET4). The scanner is made of 32 avalanche photodiode detector rings and produces 63 image planes (32 direct, 31 cross) over a 3.75 cm axial field of view (FOV). The pixel size after reconstruction is 0.5mm×0.5mm×1.175 mm. The scanner h

as a flexible system of acquiring list-mode data that allow elaborate dynamic PET image series to be extracted as desired. Almost 60 minutes of dynamic acquisitions in list-mode were performed on the LabPET4 scanner. Radiotracer was injected via a catheter in the caudal vein. The injection of 50 ± 5 MBq of ^{18}F-FDG in a volume of 400 µL was done over the course of 1 minute using an automatic infusion pump in the tail vein. During the acquisition, blood was withdrawn through a femoral artery catheter at 20, 40, 50, 60, 70, 90, 120, 150, 180 sec and at 5, 10, 15, 20, 25, 35, 52 min. The blood time-activity curves were generated from a linear interpolation of the blood sampling data to the PET dynamic series of 31 frames. Thirty minutes after the injection, the glucose level was obtained from the plasma analysis using a commercial reagent kit (Siemens Healthcare Diagnostic Inc., Deerfield, IL, USA) and an automated clinical chemistry analyzer (Dimension Xpand Plus, Siemens Healthcare Diagnostic Inc., IL, USA).

B. Methods

In order to quantify the MMRG, a mathematical framework was developed by several investigators [4,5]. The three-

compartment ^{18}F-FDG model is utilized in this study for estimating the rate constants and the MMRG. The model which refers to the target tissue measured by the scanner is described by a set of differential equations where the solution is given by the following [5]:

$$C_T(t) = \Big(C_f(t) + C_m(t)\Big) + \vartheta C_b(t), \quad (1)$$

where

$$C_f = \left(\frac{K_1(k_4-\alpha_1)}{\alpha_2-\alpha_1}[(k_4-\alpha_1)e^{-\alpha_1 t} + (\alpha_2-k_4)e^{-\alpha_2 t}]\right) \otimes C_p,$$

and

$$C_m\left(\frac{K_1 k_3}{\alpha_2-\alpha_1}\left[e^{e^{-\alpha_1 t}} - e^{-\alpha_2 t}\right]\right) \otimes C_p$$

with

$$\alpha_1, \alpha_2 = \frac{\left[k_2+k_3+k_4 \mp \sqrt{(k_2+k_3+k_4)^2 - 4k_2k_4}\right]}{2}$$

and C_p is the parent tracer concentration in plasma. It refers to the IF in the model. C_b is the whole blood concentration. C_T, C_f and C_m are respectively the total tissue concentration, the extracellular concentration and phosphorylated FDG concentration. The constant K_1 refers to the rate of delivery of the tracer to tissue in units of volume of blood per mass of tissue per minute (mL/g/min), and k_2, k_3, k_4 are the transport rate constants in units of min^{-1}. The symbol $\otimes$ in (1) indicates the convolution operation. The MMRG is defined by:

$$MMRG(\mu mole/100g/\text{min}) = 100\frac{gl}{LC}K \quad (2)$$

where gl is the glycemia value in $mmol/L$, $K = \frac{k_1 k_3}{k_2+k_3}$ the influx rate constant and $LC = 1$ is the lumped constant accounting for the utilization of FDG versus glucose which is the natural substrate.

In order to correct blood and tissue for the cross contamination, we propose in this paper a new likelihood function for tissue and blood activities and one for *a priori* knowledge of the blood activity in the Bayesian approach presented in [3]. Given two manually drawn region of interest (ROI) as depicted in Figure 1(first one around the blood pool and second one around the myocardium),

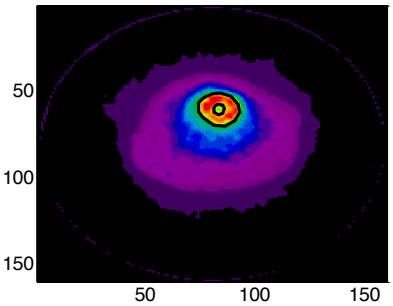

Figure 1- Image of the rat heart measured with ^{18}F-FDG during 20 min at 40 min after tracer injection

we denote the region delimited by the external contour in image as S. The pixels outside this region were not considered for cross contamination correction. The activity within S is modeled as a random field X^t, where $t = 1, \cdots, \tau$ refers to the time index of the image frame within the sequence. The value of X^t at a point $s \in S$ is written as: x_s^t. We consider every frame measurement as a mixture of two distinct components for blood and tissue activities. Consequently, X^t is modeled as a mixture of two random processes, X_B^t which models the blood component and X_T^t which models the tissue component. S is spatially split into two parts, S_B and S_T. Thus, we consider that the pure activity of blood into the manual ROIs is given by :

$$x_{B,s}^t = \begin{cases} \alpha_{B,s}^t\, x_s^t\,, & s \in S_B \\ \left(1-\alpha_{T,s}^t\right) x_s^t, & s \in S_T, \end{cases} \quad (3)$$

and the pure activity of blood into the manual ROIs is given by :

$$x_{T,s}^t = \begin{cases} \left(1-\alpha_{B,s}^t\right) x_s^t, & s \in S_B \\ \alpha_{T,s}^t\, x_s^t\,, & s \in S_T \end{cases} \quad (4)$$

In (3) and (4), $\alpha_{B,s}^t \in [0,1]$ and $\alpha_{T,s}^t \in [0,1]$ are the actual fractions of blood and tissue activities at each pixel $s \in S$ at time $t = 1, \cdots, \tau$. In the following, we estimate these fractions from the measured X^t using a Bayesian framework as :

$$\alpha_{B,s}^t \overset{\text{def}}{=} p(X_B^t | x_s^t).$$

Using the Bayes' rule one obtains

$$\alpha_{B,s}^t = \frac{p(x_s^t|X_B^t)\, p(X_B^t)}{\sum_{i=B,T} p(x_s^t|X_i^t)\, p(X_i^t)}, \quad (5)$$

Similarly, the tissue fraction is defined as:

$$\alpha_{T,s}^t \overset{\text{def}}{=} p(X_T^t | x_s^t),$$

then

$$\alpha_{T,s}^t = \frac{p(x_s^t|X_T^t)\, p(X_T^t)}{\sum_{i=B,T} p(x_s^t|X_i^t)\, p(X_i^t)}, \quad (6)$$

where $p(x_s^t|X_B^t)$ and $p(x_s^t\,|X_T^t)$ are modeled by a GGD. The functions $p(x_s^t|X_i^t)$ for $i = B\ or\ T$ are given by:

$$p(x_s^t|X_i^t) = \frac{\beta_i}{2\sigma_i\Gamma\left(\frac{1}{\beta_i}\right)} e^{-\left[\frac{|x_{s,i}^t-\mu_i|}{\sigma_i}\right]^{\beta_i}} \quad (7)$$

where $x_{s,T}^t$ is a pixel belonging to the tissue ROI. The estimation of the different parameters $(\mu_i, \sigma_i, \beta_i)$ is presented in [6]

The *a priori* for the blood is computed from a sampled C_p curve. The curve was carefully sampled with a 5 seconds step during the first 2 min of the scan. The weights over time in the Bayesian rule are calculated as follows:

$$p(X_B^t) = \begin{cases} 1 & \text{if t}\leq 2\text{min} \\ \dfrac{\text{SC}_\text{p}}{\sum \text{SC}_\text{p}} & \text{if t}>2\text{ min}, \end{cases} \quad (8)$$

Where SC_p is the sampled C_p. Figure 2 depicts the blood prior $p(X_B^t)$

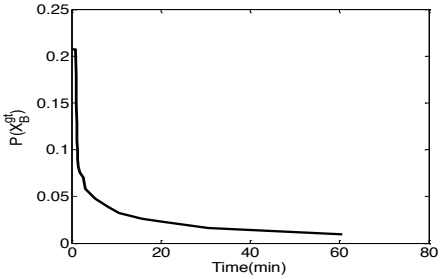

Figure 2- Prior probability of $p(X_B^t)$ after a bolus injection, the tracer diffuses into the tissue and consequently it exponentially decreases with time.

The tissue prior $p(X_T^t)$, depicted in Figure 3, is computed from the FDG model as the response of tissue after a bolus injection. It follows from (2)

$$p(X_T^t) = \frac{k_1}{\alpha_1+\alpha_2}\left[(k_3+k_4-\alpha_1)e^{(-\alpha_1 t)}(\alpha_2-k_3 - k_4)e^{(-\alpha_2 t)}\right] \otimes p(X_B^t) \quad (9)$$

where k_1= 0.102 ml/ min/ g , k_2 = 0.13 min^{-1}, k_3 = 0.062 min^{-1}, and k_4= 0.0068 min^{-1}. These parameter values are representative of those usually obtained from studies in normal subjects.

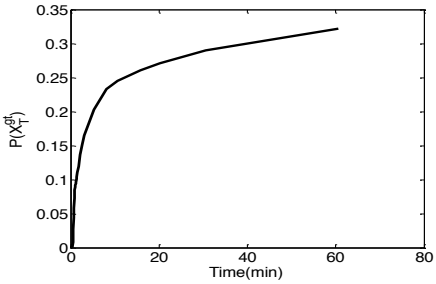

Figure 3- Prior probability of $p(X_T^t)$. The PET measurement in a tissue is viewed as the cumulative uptake response of the radiotracer diffused by blood

III. Results

Our approach allows to isolate the fractions of blood and tissue in each pixel of the PET image. Consequently, it allows to generate blood and tissue image sequences with low cross contamination. The ROI's mean calculated on each image sequence produce free cross contamination effect time activity curve (TAC). Figure 4 depicts TACs calculated by different technic on the same subject.

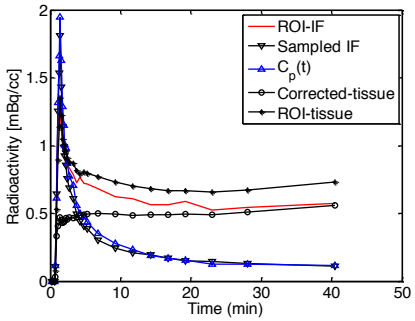

Figure 4-time activity curve calculated from the same rat. Comparison between sampled, extracted IF (C_p) and IF from ROI shows that the ROI-IF is higher than the sampled and the extracted is close to the sampled.

To assess the macroparameter MMRG, One common method uses just one tissue TAC and equation(1). Figure 5 illustrates kinetic modeling using (1).

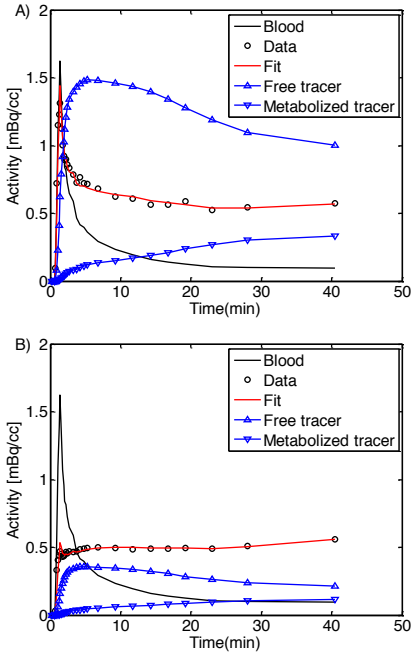

Figure 5-. A nonlinear least squares fitting of the f tissue TAC by the three compartment model. (A) tissue TAC is computed from original image as a mean of tissue ROI acitivies. (B) tissue TAC is computed from corrected image as a mean of tissue ROI acitivies

Figure 5(A) shows an early peak in tissue and consequently, the fit of real data give by nonlinear least squares would not allow a reliable parameters. In contrast, in Figure 5(B) the second term in (1), which refers to the fractional contribution

of blood in tissues, is insignificant. This is a result of the correction made in the tissue activity over the time.

However, the global MMRG assessment is not a reliable method to study the viability of different areas of the heart. The method is used as an indicator of the global function of the organ. In contrast, the production of MMRG value at each voxel allows a good prediction of the viability of the tissue. Figure 6 depicts a parametric images calculated with and without correction of the tissue activity. In Figure 6(A) the unit of glucose metabolism is poorly visualized due to the effect of the cross contamination of tissue TAC activities on the original image. In contrast, Figure 6 (B) illustrates the importance of correcting for tissue activity. Indeed, the parametric image has a good contrast and the estimated MMRG values appear as expected for a healthy heart.

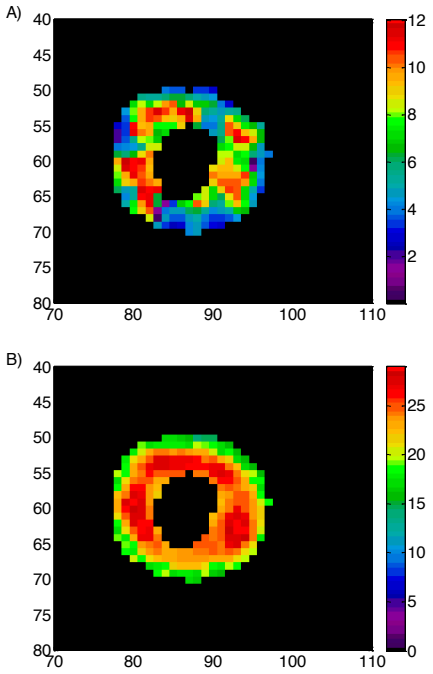

Figure-6: Parametric MMRG image. Images are resized directly in units of glucose metabolism (micromole/100g/min). (A) Parametric MMRG image computed with original images. (B) Parametric MMRG image computed with corrected images.

In the case of MI induced by ligature of the left coronary artery which delivers glucose to the myocardium, we expect to obtain a lower unit of MMRG on the parametric image. Figure 7 illustrates glucose uptake pixel-by-pixel calculated on corrected and uncorrected tissue activity. Figure 7(A) illustrates the effect of cross contamination on the calculated MMRG value. The contrast is lower than the image calculated with corrected tissue TAC in Figure 7(B) which depicts clearly the area of the extent of damaged tissue.

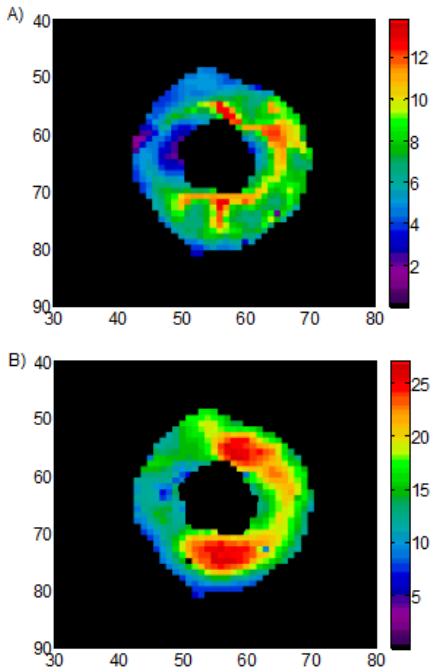

Figure 7- Parametric MMRG image for infarcted heart. (A) Parametric MMRG image computed with uncorrected images. (B) Parametric MMRG image computed with corrected images.

IV. Conclusion

We showed that the probabilistic estimations of the blood activity and the tissue activity in this work have an important benefit in the production of parametric images. Moreover, the MMRG parametric image has the advantage making easy the numerical evaluation of myocardial metabolism, and the compression of several image frames of dynamic PET studies.

References

[1] Wu HM, Hoh CK, Choi Y, Schelbert HR, Hawkins RA, Phelps ME, Huang SC, "Factor analysis for extraction of blood time-activity curves in dynamic FDG-PET studies," J Nucl Med, vol. 36, pp.1714–1722, 1995.

[2] K.H. Su, J.S. Lee, J.H. Li, Y.W. Yang, R.S. Liu, and J. C. Chen, "Partial volume correction of the microPET blood input function using ensemble learning independent component analysis," Phys Med Biol, vol. 54, pp.1823–1846, 2009.

[3] R. Mabrouk, F. Dubeau, M. Bentourkia, and L. Bentabet "Extraction of time activity curves from gated FDG-PET images for small animals' heart studies". Comput Med Imaging Graph vol 36, pp. 484-491, 2012.

[4] Patlak CS, Blasberg RG, Fenstermacher JD. Graphical evaluation of blood-to-brain transfer constants from multiple-time uptake data. J Cereb Blood Flow Metab, vol 3, pp 1–7, 1983.

[5] Phelps ME, Huang SC, Hoffman EJ, Selin C, Sokoloff L, and Kuhl DE. Tomographic measurement of local cerebral glucose metabolic rate in humans with (F-18)2-fluoro-2-deoxy-d-glucose: validation of method. Annals of neurology, vol 6, pp 371–388, 1979.

[6] Mabrouk R, Dubeau F, Bentabet L. Dynamic Cardiac PET Imaging: Extraction of Time-Activity Curves using ICA and a Generalized Gaussian Distribution Model. IEEE- Tran on Biomedical Engineering , vol 60, pp 63-71, 2013.